Environmental Technology and Innovation, Volume 21, February 2021, Article number 101350
DOI:10.1016/j.eti.2020.101350

Recycling of waste coal dust for the energy-efficient fabrication of bricks: A laboratory to industrial-scale study

Milica Vidak Vasić[a,*], Gaurav Goel[b,c], Miloš Vasić[a], Zagorka Radojević[a]

[a]*Institute for Testing of Materials IMS, Bulevar vojvode Mišića 43, 11000 Belgrade, Serbia*

[b]*School of Engineering, London South Bank University, 103 Borough Road, London, SE10AA, UK*

[c]*School of Aerospace, Transport and Manufacturing, Cranfield University, MK430AL, UK*

*Corresponding author. *E-mail address:* milica.vasic@institutims.rs (M. V. Vasić)

Abstract

In this study, an optimal mixture of loess brick clays and waste coal dust in laboratory hollow blocks production is determined with the aim of promoting sustainable development in terms of saving resources and energy. The novelty of the work lies in the first-time utilization of waste coal dust in combination with loess soil brick-making thus bolstering European effort on waste utilization. The mentioned is also in line with UN sustainable development goals, SDG 12 and 9. The chemical and mineralogical contents of the clays were obtained using various chemical characterization methods, and thermal behavior by using dilatometry and simultaneous DSC/TG analysis. The important ceramic and technological characteristics of the extruded brick clay and waste coal dust composite samples during molding, drying, and firing were obtained. The chosen mixture of 70 % calcareous clay and 30 % plastic clay to 3 % of high-calorie waste coal dust is found optimal. Industrial-scale optimal blocks (250x190x190 mm^3) with 60 % of vertical voids were fired in a tunnel kiln, and the firing regime was recorded. It is determined that the regime must be corrected in the firing and cooling zone since the differences measured by thermo-couples were up to 180 °C. The industrial prototype was found to be of satisfactory quality meeting the requirements of water absorption and compressive strength as per European and other international standards. The study was first of a kind detailed characterization of the industrial size bricks encompassing

waste coal dust and loess brick clays, with the emphasis on the usability in the industry, and additionally recording and correcting of the firing regime in a tunnel kiln. The product is recyclable and can be disposed of safely after the end of life.

Key words: Loess brick clay; Coal dust; Optimal mixture; Tunnel kiln; Firing regime; Optimization

1. Introduction

Thermal power plants are considered the main sectors in the economy of Serbia. In terms of the annual production of lignite, Serbia ranks 10th in the world. The estimated reserves of this coal are 10 % of the total in Europe. About 40 million tons of lignite are extracted daily in the country for electric power generation. Although it is the greatest treasure in the region, lignite could prove to be the most prominent problem. Being low-caloric and with huge moisture content, lignite is the worst quality coal - it has low thermal power, leaves a lot of ash when burned, and leads to increased gas emissions (such as CO_2 and SO_2). Many studies presented the possibility of using fly and landfill ashes in different applications, but only 3 % of total ashes are spent in the cement industry in Serbia, while the brick industry avoids using it (Arsenović et al., 2015a; Gupta, 2017; Vukićević et al., 2018). Besides, there is no published research on using coal washery rejects such as waste coal dust in the country, and it is not even considered a valuable waste (Vijayan and D. Parthiban, 2020).

Throughout coal mining and washing, the waste remains in up to 15 % (Haibin and Zhenling, 2010). The coal is washed to improve its quality, in which process large amounts of water are used, and the leftover material containing impurities is discarded. Since the demand for coal as fuel is huge, a significant quantity of waste is generated during mining and handling activities. The generated waste is among the prominent environmental problems. Fortunately, the washery rejects are used in many sectors such as the construction industry, as underground backfill material, or reused as energy-containing matter (Fan et al., 2014; Li and Wang, 2019), etc. The studies concerning the usage of coal production reject in the ceramic industry are scarce. Coal mine waste rocks and treated coal mine tailings, containing soil and leftover coal dust, were used to produce 50 % or 100 % eco-friendly bricks (Abi et al., 2011; Lemeshev

et al., 2004; Taha et al., 2016). It is shown that coal mining and processing waste can be successfully used in wall tiles production in quantities up to 80 % (Stolboushkin et al., 2016). Only two studies in literature used waste coal dust in brick making. The first one showed that waste coal dust can be optimally added in a quantity of 10 wt % to produce hand-molded bricks fired at 1000 ºC with increased compressive strength and reduced water absorption compared to the pure clay bricks (Gökçe et al., 2018), but the more detailed research is needed. The other work reported that the addition of dry waste coal dust in a quantity of 3 % and 6 % in plastic clay is optimal for the production of hollow blocks (Arsenović et al., 2015b), yet there is the need for testing the possibility of using loess soil as the base material.

Loess soils are not amongst the highest quality raw materials in the brick industry, and, as such, are rarely studied. They are characteristic for high contents of carbonates and alevrolite-sized fraction, but also a sequence of the buried soil rich in clay minerals. This material can be generally used in the production of bricks without cavities but also can be enriched to produce modern energy-efficient hollow blocks (Arsenović et al, 2014; Vasić et al., 2020). The important fact is that the deposits consist of a lesser quantity of the buried soil (high contents of clay minerals and lack of carbonates) in comparison to the calcareous clay.

The possibility of mixing waste into the soil to produce bricks has been frequently explored during the last decades at a global level. The studies intend to manufacture bricks with the improved porosity, and thus lowered thermal conductivity, bearing in mind the possibly increased carbon footprint. Besides, the savings in energy and natural raw material are not to underestimate. Decreasing the plasticity of the mix and possible uncontrolled release of energy throughout the firing are the main concerns when designing the proper mixtures with different components (Arsenović et al, 2015a; Bocanegra, 2019; Goel et al., 2018).

In this study, the composites of dry waste coal dust and loess brick clay are for the first time analyzed in detail, and the mixture is optimized. It is hypothesized that the addition of waste coal dust would improve the energy-efficiency of loess clay bricks while firing at the same peak temperature and that the developed industrial products will satisfy the corresponding EN norms. Besides, this study presents scaling up to the production in the factory and correction of the firing regime in a tunnel kiln. It is concluded that waste coal dust of 7.6 MJ/kg calorific value can be safely added in a

quantity of 3 % to loess calcareous clay, thus obtaining a 60 % of voids industrial thermo-block.

2. Materials and methods

This section is focused on the characterization of the constituent materials and reports on the scheme to obtain different mixes. Drying, moulding, and firing methods are elaborated in detail. Finally, the procedure to obtain an industrial scale specimen is described.

2.1. Characterization and preparation of the raw materials and mixtures

In this study, 2 primary loess brick clays (BC1 and BC2) from Vojvodina, Serbia were used to make mixtures with waste coal dust as an eco-friendly raw material in the brick industry. The clays (BC1 and BC2) were mixed in different proportions to make 2 additional clays (BC3 and BC4). The coal dust, from the washing process of coal, is taken off the filters from a coal washery. Two types of dust were used: one of a higher calorific value and lower moist (CD1), and the other of lower calorific value and higher moist content (CD2). The appearance of the as-received samples of waste coal dust can be seen in Fig. 1, where All percentages refer to the dry weight of both raw materials - brick clays and waste coal dust samples.

Fig. 1. The appearance of coal dust: (a) CD1, and (b) CD2.

The used experimental design is schematically presented in Fig. 2. It seems that the waste coal dust samples were similar besides the particle sizes, both containing coarse and small white grains.

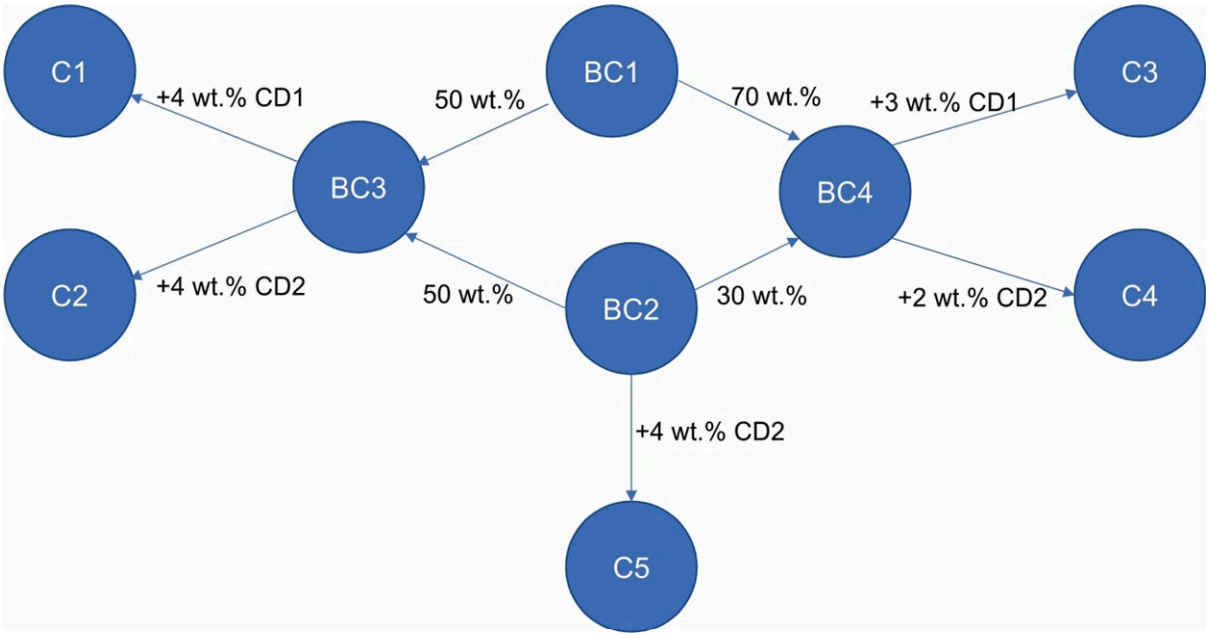

Fig. 2. Schematic representation of the tested brick clays (BC) and waste coal dust (CD) mixtures to obtain C1-C5 composite materials.

The particle size distribution of the primary clay and dust materials is determined on as-received samples, while the mixtures containing waste coal dust were tested for granulometry after the grinding of CD1 and CD2 to fractions below 1 mm. The method used for testing was a combination of hydrometry (for particles below 0.063 mm) and wet sieve analysis according to the procedure described in the standard (SRPS U.B1.018). The samples pre-dried at 105 °C were sieved through the standard sieves, and the remains on each sieve were measured with an accuracy of 0.1 wt.%. The solution of sodium hexametaphosphate was used as a dispersing agent (anticoagulant) of the fine-grained particles. The particle size ranges for the indicated particle sizes classes were clay (< 0.002 mm), alevrolite (0.002 mm – 0.06 mm), and sand (0.06 mm – 2 mm) (Kovács et al., 2006).

The primary samples of brick clays (BC1 and BC2) were dried in an oven at 105 °C to a constant mass and subsequently dry-ground in a mill with a gap of 3 mm. The chemical and mineralogical compositions of the clays BC1 and BC2 is determined using the energy dispersive X-ray fluorescence (XRF) technique (Spectro Xepos; 50

W / 60 kV X-ray tube) and X-ray diffraction (XRD) analysis (Philips 1050; Ni-filtered CuK_α radiation of $\lambda = 1.5418$ nm and Bragg–Brentano focusing geometry, 6 – 90 ° 2Θ range with the step of 0.05°, the exposure time was 6 s per step). The waste coal dust samples (CD1 and CD2) were also dry-ground and the fraction passing the 1 mm sieve is used in the mixtures. The macro and microelements contents in coal dust ash are determined by XRF analyses.

The raw materials and mixtures were tested for thermal behavior using differential scanning calorimetry and thermal gravimetry (SDT Q600, TA Instruments; the flow of air 100 cm^3/min, the heating rate 20 °C/min up to 1000 °C) and dilatometry (Seteram instrument; the air atmosphere with a 20 ml/min flow, the heating speed 20 °C/min, the soaking time 1h).

2.2. Molding and drying behavior of the laboratory samples

After the initial preparation of the raw materials, the dry mixtures were made following the experimental design defined in Fig. 2. Then, the materials were moistened and left to rest for 24 h in sealed nylon bags for moisture homogenization. Before molding, the moist samples were passed through a pair of rollers with a 0.5 mm gap for further homogenization of the moisture, but also the particle sizes. The extrusion process is done under a vacuum in a laboratory Händle machine. The samples in the form of 120x50x14 mm^3 tiles, 55.3x36x36 mm^3 hollow blocks, and 30x30x30 mm^3 cubes were produced. The tiles mimicked roofing tiles, the cubes were representative of a common brick without voids, and hollow blocks were of proportional measures to industrial products containing about 50 % of voids. Afterward, the samples were gently dried until 105 °C to finally obtain the constant mass requirement.

The wet samples were used to test the sensitivity to drying by Bigot and plasticity coefficient according to the method by Pfefferkorn (Arsenović et al, 2014). The green (dry) samples were used to determine the remainings on the sieve (RS) of 0.063 mm by the wet procedure and the amount of total calcium and magnesium carbonates (CCC) by a volumetric method (Scheibler`s calcimeter) (Arsenović et al, 2014). CCC was also determined in the samples of coal dust.

Shaping moisture (SM) was determined in all kinds of molded samples and the average value is presented, while drying shrinkage (DS) is measured using the tiles. The parameters are determined as a percentage difference between wet and dry

samples in mass and length. The accuracy of the scale and caliper were to the second decimal place.

The flattened laboratory samples having parallel sides were tested on an Alfred Amsler hydraulic machine by which the compressive strength of the hollow blocks (CSBD) and cubes (CSCD) is determined as an average value of the 3 samples. It is taken care that the measured force is the one needed for the complete crash of the samples, as required by the standard (SRPS EN 772-1).

2.3. The firing of laboratory samples

The firing was conducted in an electric laboratory oven in oxidizing conditions. The chosen firing temperatures were 950 °C,1000 °C, and 1050 °C. The slow-firing regime is followed, and the soaking time was 2 h (Vasić et al., 2018). The cooling was performed in natural conditions in a closed furnace.

The samples were measured for determination of loss on ignition (LOI) and firing shrinkage (FS) immediately after the removal from the furnace. The weight measurement was conducted on a scale with a precision of 0.01 g, while the caliper used had 0.01 mm accuracy.

Bulk density (BD) and water absorption (WA) were determined in the standard-defined ways (SRPS EN 772-13, SRPS EN 772-21).

The compressive strength of the laboratory fired hollow blocks (CSB) and cubes (CSC) is determined as described in *Section 2.2.*

2.4. Industrial probe

After defining the optimal mixtures of the loess clays and two waste coal dust samples, the industrial probe is done. The raw materials are mixed and a mound is made to homogenize the material and the moisture. The primary processing involved grinding below 1 mm. Larger concretions of carbonates (> 1 mm) require a special processing line in the industry, with purifier and grinding in several stages so that they do not remain in the form of CaO after firing. Due to hydration during the transition of CaO to $Ca(OH)_2$, there is an increase in volume, and then by binding CO_2 from the air, $CaCO_3$ is formed, which reaches about three times the volume of the initial CaO. These reactions cause frequent "popping" and even damage to the product. The

blocks with about 60 % of vertical voids (250x190x190mm^3) are made by the extrusion process and tested for shaping moisture, plasticity coefficient, sensitivity to drying, and remains on the 0.063 mm sieve (the methods explained in *Section 2.2*).

A multi-channel acquisition system THERM 3256-6 (Ahlborn Mes und Regelungstechnik), and 8 flexible NiCr-Ni thermocouples (type K), manufactured by OMEGA, were used in the tunnel kiln firing regime diagnostic process. Thermo-couples are placed in the lower, middle, and upper rows of the middle of the stack from below through the wagon.

The compressive strength of the industrial probes is determined after flattening the blocks` surfaces using mortar (SRPS EN 772-1), in the hydraulic press Tonindustrie, Germany with a maximum force of 2000 kN. Water absorption is measured according to SRPS EN 772-21:2012. Pre-dried samples are immersed in cold water for 24 ± 0.5 h. The mass of the dry and soaked samples is measured with an accuracy of 0.1 %. The results of water absorption are presented relative to the mass of the dry sample.

3. Results and discussion

Properties of the lab- and industrial-scale bricks are determined in this section and results are reported. The quality of these products is then determined and found satisfactory meeting European norms.

3.1. Characteristics of the raw materials

The macro-oxides composition of the primary brick clays, as determined by XRF, is shown in Table 1. The main difference between the primary clays was the carbonates: the sample BC1 contained high concentration and belonged to calcareous clays (Taalab et al., 2019), while the sample BC2 showed a relatively low content of calcite and magnesite. Besides, the clay BC1 contained more of a silt fraction and belonged to silty loam (Fig. 3), while BC2 was a member of silty clay loam. It is concluded (Fig. 3) that all the mixtures prepared were of similar granulometry as primary raw materials (BC1 and BC2). The mixtures of the primary loess clays (BC3 and BC4) fell into a group of silty loam. Based on the results of these laboratory tests, it can be concluded that the brick clay raw materials belonged to silty sediments

252 contaminated with carbonates. Carbonates are found in the raw material mainly in
253 finely dispersed form, with a rare appearance of limestone concretions.
254

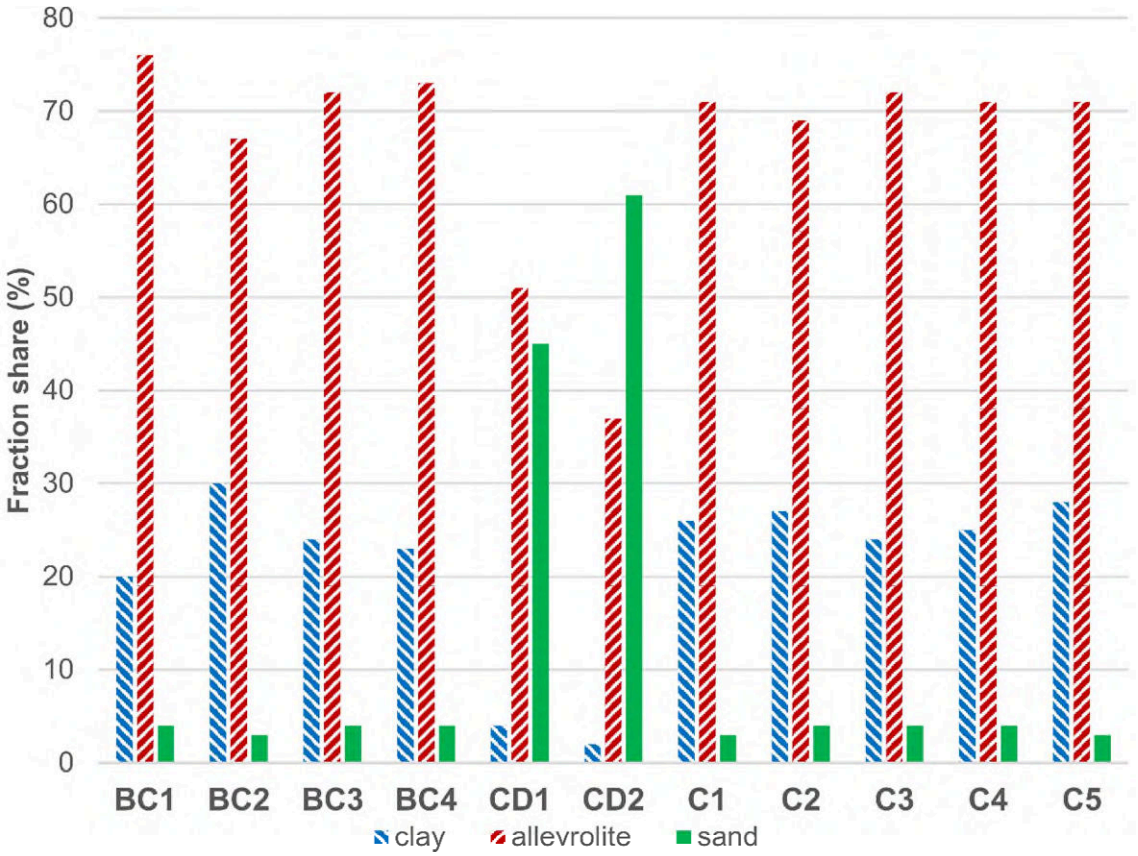

255
256 **Fig. 3.** Granulometry analysis of the samples prepared for molding.
257
258 The basic difference between the waste coal dust samples was in calorific
259 values and moisture contents, as seen in Table 2. CD1 and CD2 showed
260 approximately half the calorific value of lignite coal (Özdemir and Sarici, 2020). The
261 XRF analysis of dried CD1 and CD2 is shown in Table 3. The content of ash was
262 relatively high (Chen et al., 2015; Lingam et al., 2016), and the waste samples mostly
263 contained SiO_2, Al_2O_3, Fe_2O_3, and CaO. Considering the microelements contents, and
264 the EPA regulations, this waste is not hazardous, nor it can leach out from the final
265 brick product.

Table 1

Chemical composition of the brick clays.

	SiO_2 (%)	Al_2O_3 (%)	Fe_2O_3 (%)	CaO (%)	MgO (%)	Na_2O (%)	K_2O (%)	SO_3 (%)	P_2O_5 (%)	MnO (%)	TiO_2 (%)	LOI (%)
BC1	50.69	12.54	3.95	9.34	5.89	1.49	1.44	0.03	0.18	0.09	0.66	13.72
BC2	62.25	15.26	4.70	1.21	3.47	1.53	2.26	0.03	0.12	0.12	0.76	8.37

Table 2

Important characteristics of the waste coal dust samples.

	Clay-sized fraction (%)	Alevrolite-sized fraction (%)	Sand-sized fraction (%)	Content of moisture (%)	LOI (%)	Total contents of carbonates (%)	Ash content (%)	Calorific value (kJ/kg)	Maximum dry addition (%)
CD1	4	51	45	50.7	34.5	0.0	14.8	7569	4.62
CD2	2	37	61	56.3	29.5	0.0	14.2	6188	5.66

272 **Table 3**

273 XRF analyses of coal dust.

Sample	CD1	CD2
LOI (%)	76.77	64.04
SiO_2 (%)	13.67	21.10
Al_2O_3 (%)	4.36	7.72
Fe_2O_3 (%)	1.61	2.04
CaO (%)	2.09	2.41
MgO (%)	0.78	1.06
Na_2O (%)	0.19	0.29
K_2O (%)	0.33	0.65
SO_3 (%)	0.03	0.33
P_2O_5 (%)	0.02	0.04
MnO (%)	0.03	0.04
TiO_2 (%)	0.18	0.31
Ni, mg/kg	4.97	65.81
Co, mg/kg	0.98	16.90
Cu, mg/kg	1.81	37.40
Zn, mg/kg	9.04	11.76
As, mg/kg	0.30	32.44
Sr, mg/kg	53.20	70.84
Mo, mg/kg	0.67	2.59
Ba, mg/kg	8.83	222.95
Pb, mg/kg	0.28	<0.3
Sn, mg/kg	<0.3	<0.3
Bi, mg/kg	0.35	0.40
Hg, mg/kg	<0.2	0.07
Cd, mg/kg	<0.2	<0.2

274

The literature data show that the energy required for firing bricks ranges up to about 600 KJ/kg (Ferrer et al., 2015; Rimpel, 2019, Soussi et al., 2017). To roughly determine the maximum amounts of dry waste coal dust (CD1 and CD2) that could be added in the production of clay bricks, it is assumed that the amount required to compensate all the necessary energy is 350 KJ per kg of goods. The results presented in Table 2 show that the contents of dust must not exceed 5.7 % of dry mass. To be sure, the maximal addition in the laboratory probes was set to be 4 % of both waste coal dust samples. Although the sample CD1 appeared coarser because of agglomerated grains, the tests showed that CD2 was of somewhat coarser texture (Table 2). The volumetric method for determining the contents of carbonates showed that the samples CD did not contain any.

The mineralogical analysis (Fig. 4) proved the differences between the BC1 and BC2 samples according to the presence of carbonates. Based on chemical and mineralogical tests, these samples mostly contained quartz, followed by carbonates (calcite and dolomite) in BC1, a lower amount of plagioclase-type feldspar and clay minerals. Iron hydroxides and organic matter were found by DSC/TG analysis (Fig. 5a). It is revealed that the clay minerals in BC1 were mica (L), chlorite (Hl), smectite (Sm), and traces of kaolinite (K), while BC2 was the same except it did not contain K. Based on XRF, XRD, DSC, and granulometry analysis it is concluded that the higher quantity of clay minerals was present in the sample BC2.

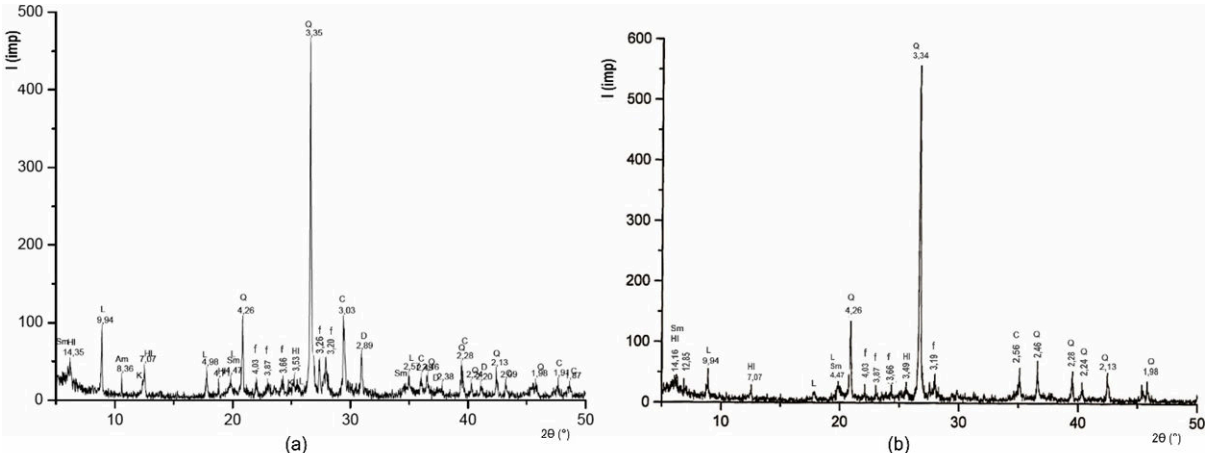

Fig. 4. Mineralogical analysis of the loess clays: (a) BC1 and (b) BC2.

From the DSC analyzes presented in Fig. 5a it is seen that the brick clays lose water with a peak up to a maximum of 74 °C (the loss of adsorbed water). Further, the

interlayer water is lost between 100 °C and 200 °C, when BC1 lost 0.39 % and BC2 0.81 % of the mass. Judging by the largest mass loss of the BC2 sample in this period, it is expected to have the slightly highest content of clay minerals (Nigay et al., 2017). At about 200 °C the organic matter decomposition begins (Arsenović et al, 2014), with the interruption by small exothermic peaks at about 270 °C -290 °C which corresponded to the transition of goethite to hematite. This reaction was the least pronounced in sample BC1 (Table 1) since the quantity of iron was the lowest (Arsenović et al, 2014). The exothermal maxima of decomposition of organics occurred at 322 °C - 339 °C. The peaks originating from the decomposition of clay minerals are overlapped by burning organic matter. A small peak resulting from quartz transformation is observed in all clays at 574 °C - 578 °C. The decomposition of organic matter took place up to about 600 °C, and the corresponding mass loss was similar in all the brick clays - about 2.6 % (Arsenović et al, 2014). Degradation of carbonates was observed in all the samples except BC2 with endothermic peaks minima at temperatures of 720 °C - 728 °C (Nigay et al., 2017). In the interval 600 °C – 800 °C, sample BC1 lost 7.36 % of the mass, while in the case of BC2 it was about 0.7 %. After 800 °C, endothermic reactions occur with small peaks at about 884 °C which could be related to the destruction of the illites` structure (Vasić et al., 2017). At the end of the test, all samples showed a small exothermic peak at 904 °C - 919 °C without the mass loss, which could be related to the formation of spinels, Fe-diopside, and/or amorphous glassy phase, since the mass loss did not occur in that period (Arsenović et al, 2014; Vasić et al., 2017), after which the endothermic processes continued. In the period from 800 ° C to 1000 °C, all the clays lost up to 0.3% of the mass.

From the DSC analyzes presented in Fig. 6a it is seen that the mixtures with waste coal dust experienced more intensive endothermic peaks than that of brick clays at the beginning of heating since the samples were not completely dry. The greatest loss of mass in the period up to 100 °C (around 3 %) and 200 °C (0.9 %) is noticed in sample C5 (around 3 %), because of high BC1 content. The exothermal process showed max peaks at about 370 °C when the mass loss was also the highest. The curves exhibited small endothermic peaks at about 380 °C, which could be a consequence of organic or maceral impurities from the waste coal dust (Ozbas et al., 2003). The complete organic matter combustion (200 °C – 600 °C) influenced the highest mass loss in C5 (6.1 %), while the lowest was observed in C4 (3.9 %). Sample

C2 showed higher content of the released energy than C1, and correspondingly the mass lost in the whole process was slightly higher (C1 – 5.1 %, C2 – 5.6 %). The addition of waste coal dust moved the exothermal maxima towards somewhat higher temperatures, compared to the brick clays alone.

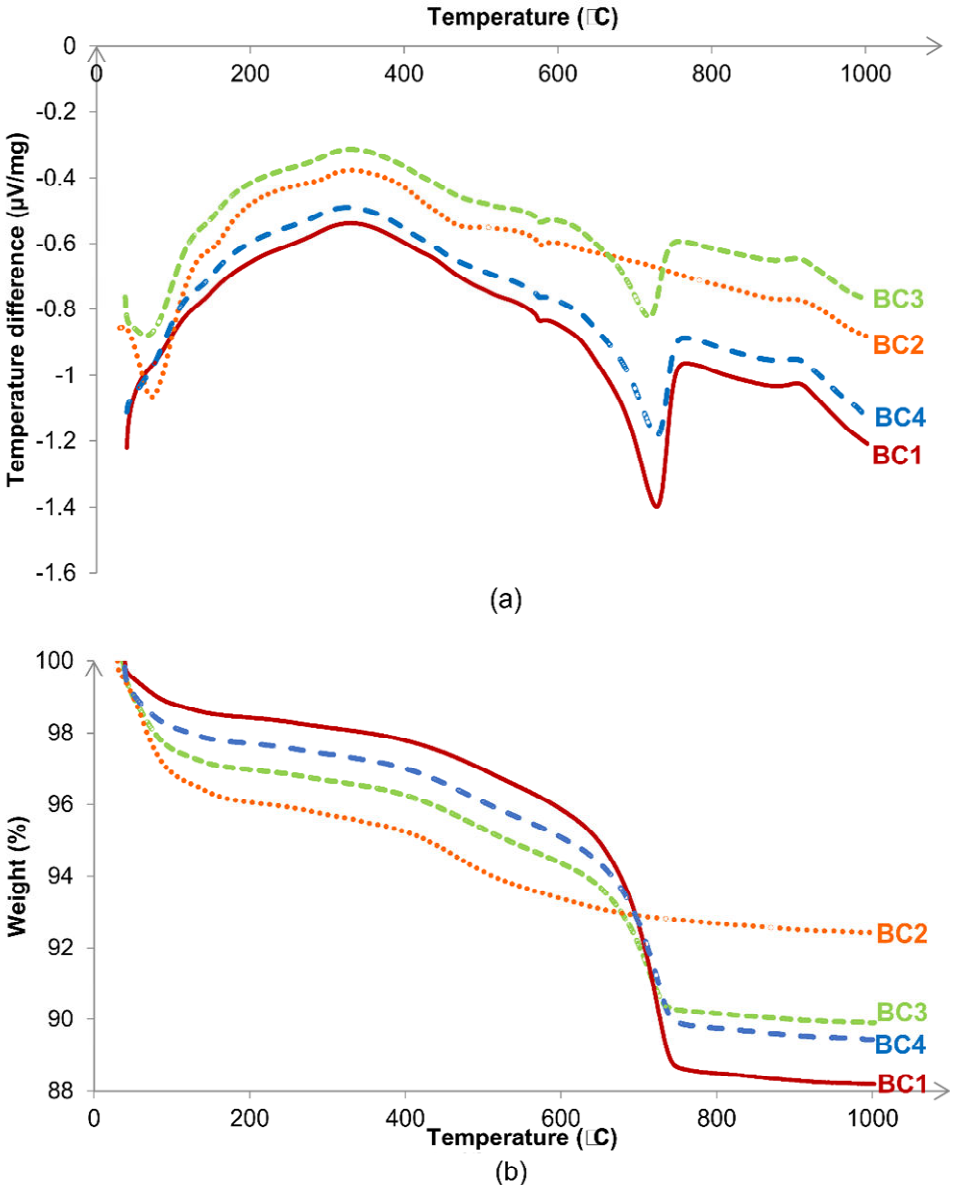

Fig. 5. Simultaneous thermal analyses: (a) DSC of brick clays, and (b) TGA of brick clays.

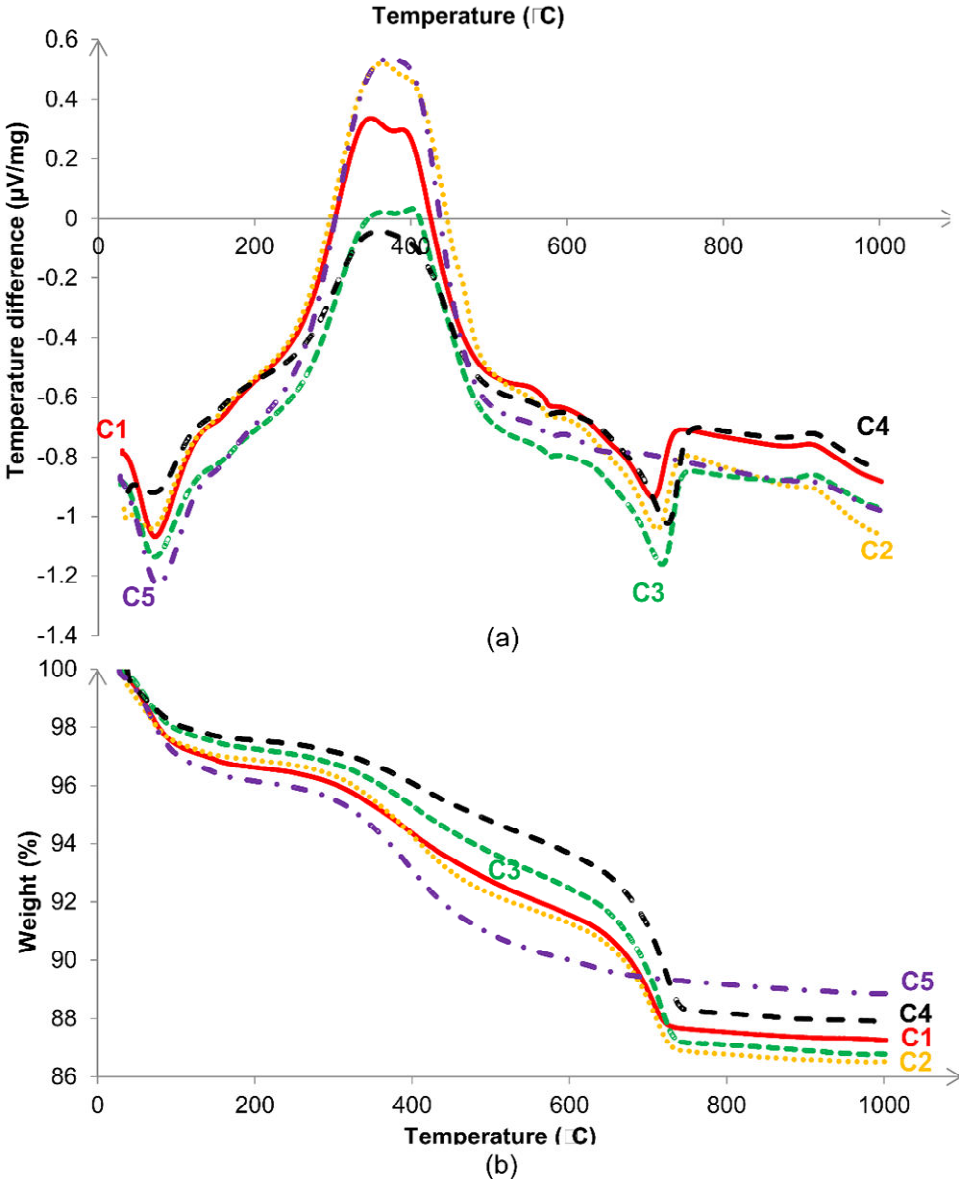

Fig. 6. Simultaneous thermal analyses: (a) DSC of brick clay-waste coal dust mixtures and (b) TGA of brick clay-waste coal dust mixtures.

Dilatometry analyses are presented in Fig. 7. The brick clays (Fig. 7a) showed similar patterns until about 640 °C. Spreading of up to about 0.2 % until 200 °C – 220 °C, caused by the water removal, is followed by a mild spread until the organic matter is released (600 °C – 620 °C), and the intensive expansion is noticed up to about 640 °C. This period is followed by a wide peak with the maximum at 890 °C in the samples BC1, BC3, and BC4, and then an intensive shrinkage due to the decomposition of illite and the formation of spinel up to 950 °C (up to about 0.4 %). Shrinkage in the mentioned samples lasted until 980 °C, and then a slight swelling occurred until the

final temperature. These then expanded during retention at 1000 °C, and the effect was the most pronounced in BC1 (about 0.3 %) and least in the case of BC3 (0.1 %).

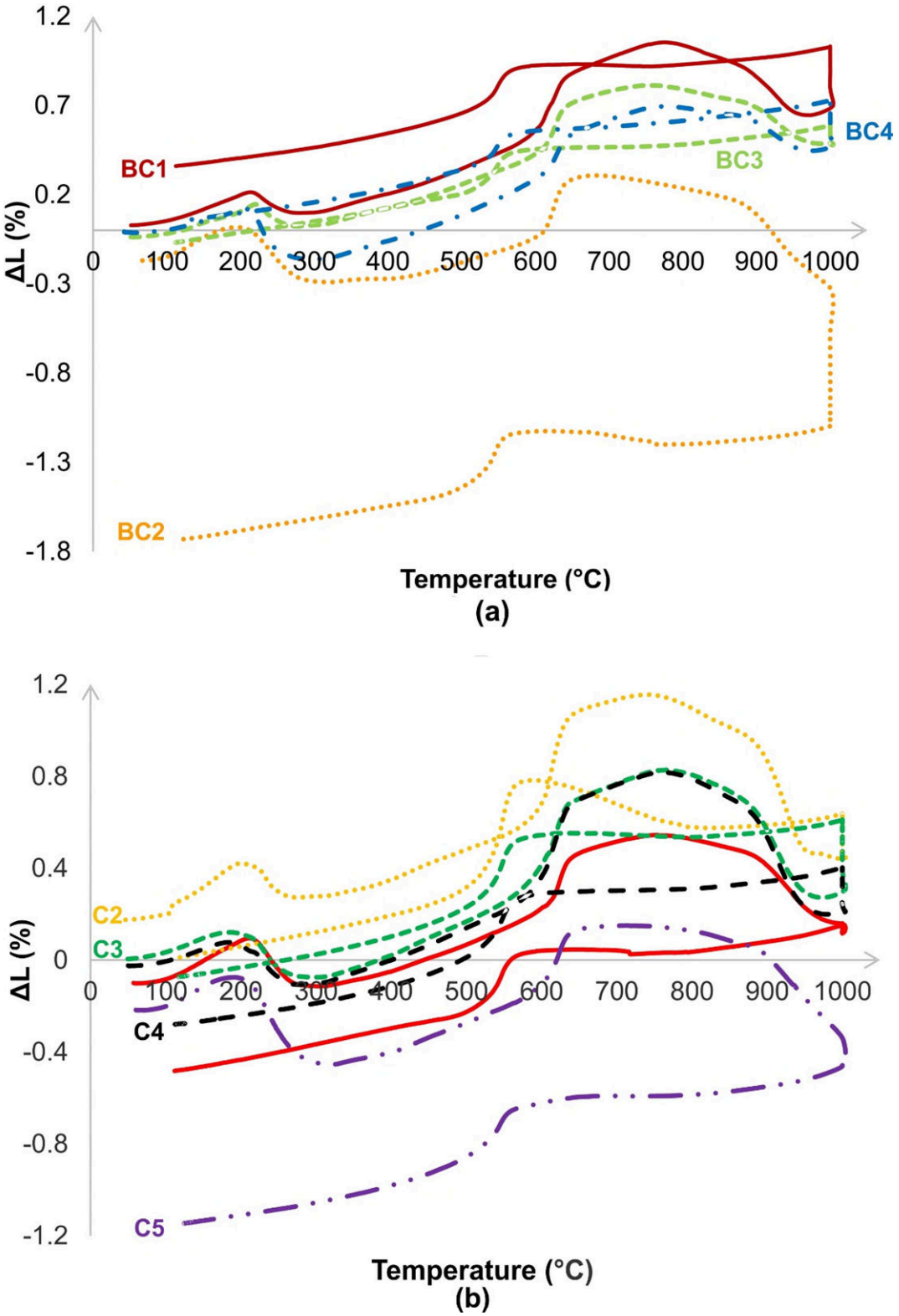

Fig. 7. Dilatometric curves of (a) brick clays, (b) clay-waste coal dust mixtures.

The expansion that occurred during the retention is rarely reported in the literature (Cobo-Ceacero et al., 2019; Pontikes et al., 2009; Rekecki et al., 2004; Vasić et al., 2017). The expansion is caused and depended mainly on the content of carbonates in the soils that contain relatively low quantities of clay minerals, since high volume anorthite may occur (Vasić et al., 2017). Besides, this effect could be influenced by the content of pure quartz (Mekki et al., 2008). The sample BC2 showed a traditional brick clay dilatometric curve (Vasić et al., 2017), with intensive shrinkage after about 900 °C, and further contraction to about 0.8 % during the retention time. The brick clay samples sintering started around 900 °C, due to the presence of illite. During the cooling period, all the brick clays showed the usual behavior, with a specific peak of quartz` conversion at about 564 °C causing the spreading in the range of 0.2 % - 0.3 %.

The mixtures of brick clays with waste coal dust represented a similar behavior to BC samples during firing (Fig. 7b). In some cases, the expansion during heating of the samples was moved toward 20 °C - 30 °C lower temperatures range when compared to the pure brick clays (C1 and C2), while in the others, there was no change in the position of the peaks. All the samples, except for C5, experienced spreading while retention at the peak temperature because of the significant presence of carbonates. After the cooling phase, the clay-waste coal dust samples shrank more than the highly calcareous BC4 clay. All the tested combinations showed sintering started after 900 °C, which corresponded to the spinel formation peaks in DSC curves (Fig.5a and Fig.6a).

3.2. The behavior of the laboratory products during molding and drying

After adequate preparation, the raw materials behaved satisfactorily during molding and were classified as materials of good plasticity according to the method by Pfefferkorn (Fig. 8). Among the clays, the sample BC1 showed the lowest plasticity since its` high content of carbonates (Vasić et al., 2017). Most of the materials were susceptible to drying according to Bigot, except for BC2 and C5 which were highly susceptible and the most plastic materials.

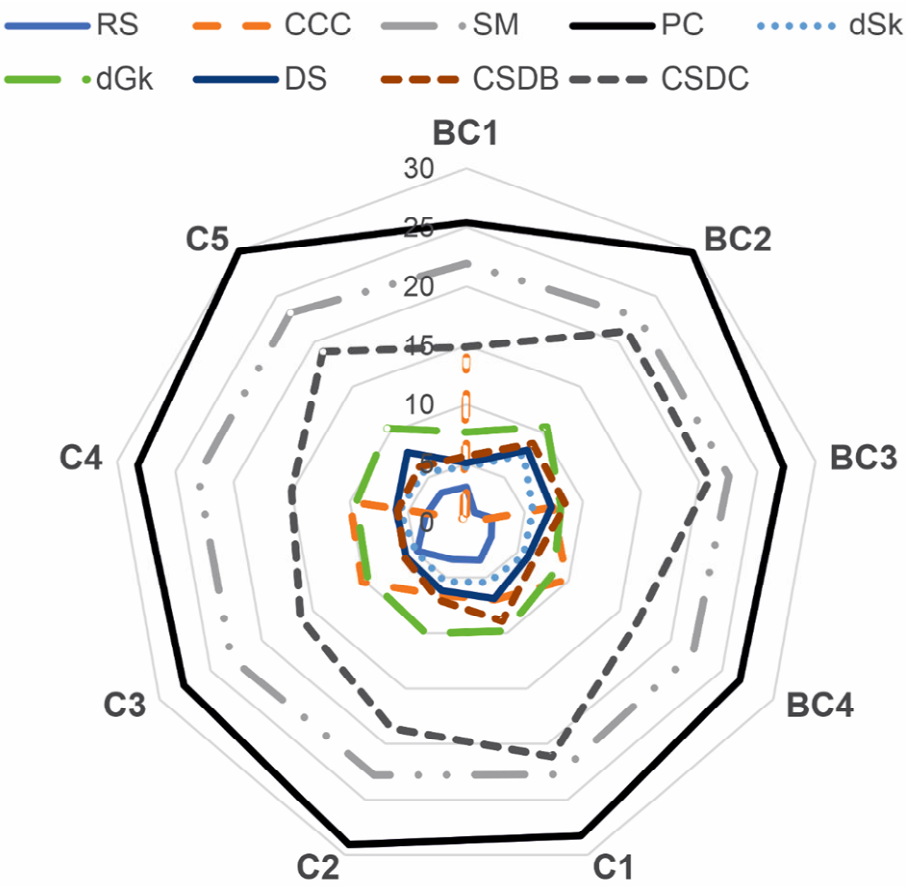

Fig. 8. Properties of the laboratory products in shaping and drying (RS – remains on the 0.063 mm sieve, CCC – total carbonates, SM – shaping moisture, PC – coefficient of plasticity, dSk – drying shrinkage in a Bigot`s curve critical point, dGk – mass loss in a Bigot`s curve critical point, DS – drying shrinkage, CSDB – compressive strength of the dry block, CSDC – compressive strength of the dry cube).

Shrinkage during drying was between about 5 % - 8 %, with the shaping moisture between 21.9 % - 23.2 %. Remains on the 0.063 mm sieve were low and varied between 1.1 % - 4.8 %, while CCC was from 0.0 % up to 14.0 %. The mechanical characteristics of the samples in the dry state were adequate, especially in the case of cubes without voids. The addition of waste coal dust somewhat increased shaping moisture, plasticity, sensitivity to drying, and total drying shrinkage. The results were comparable to the previous results (Arsenović et al., 2015b). The compressive strength of dry laboratory products was mostly reduced compared to that of the pure clay bricks, except for C1, when it slightly increased. The highest

compressive strength of clay bricks was determined for the BC2, while in dry composite products that were observed in the case of C1, C2, and C5.

3.3. Characteristics of the fired laboratory products

Some of the basic information on the fired products is presented in Fig. 9.

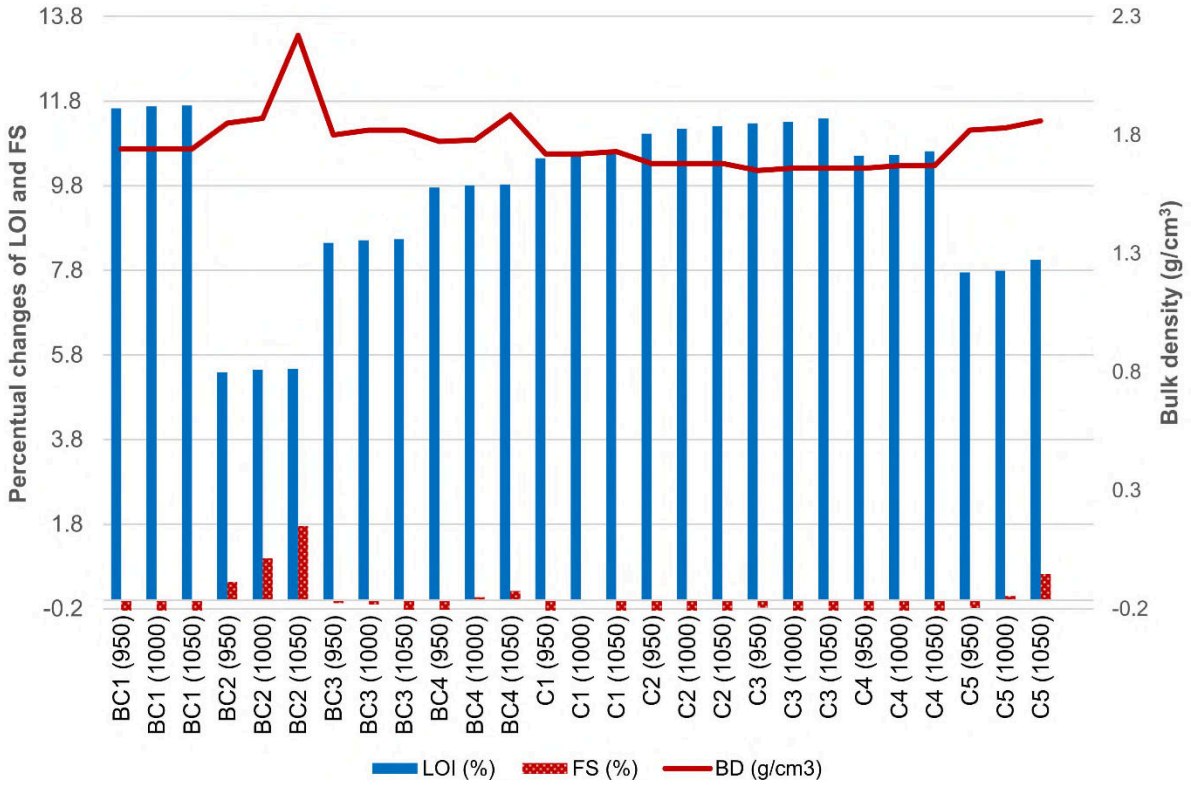

Fig. 9. Some characteristics of the products after firing at 950 ºC, 1000 ºC, and 1050 ºC (LOI – loss on ignition, FS – firing shrinkage, BD – bulk density).

It is observable that LOI slightly increases with the peak temperature and that the same is increased with the addition of coal dust. The results match the mass lost in TGA (Fig. 5b and Fig. 6b). When comparing the LOI values of C3 to C4, and BC2 to C5, it is seen that low changes in the quantity of the added waste coal dust significantly changed the behavior of samples in the firing. Firing shrinkages showed that only BC2, BC4, and C5 did not show the expansion while firing at 1000 ºC and 1050 ºC. The greatest expansion is noticed in the most calcareous BC1 samples, which was following the dilatometry analyses. The highest bulk density is obtained for BC2 and BC4 (1050 ºC), and the lowest for C3 at 950 ºC. The firing temperature

influenced BD very moderately. C5 showed the highest BD of all the coal dust-brick clay composites. FS ranged from – 0.56 % - 1.75 % in all the samples. The shrinkage was much lower than the critical 8 % (Weng et al., 2003), but the spreading should be avoided by no retention time at the peak temperature.

Laboratory samples fired at 950 °C, 1000 °C, and 1050 °C had a bright red (BC1, BC2. BC3, BC4, C3, and C4) to a brick red color C1, C2, and C5). Weak "popcorns" of lime are noticed in all the samples. Sample BC1 is considered suitable for use in the brick industry for the production of solid bricks. The addition of a more plastic clay with a higher content of clay particles BC2 (Fig.3) to the BC1 sample can enable the production of hollow products and an increase in the mechanical characteristics. By the addition of coal dust, energy-efficient products can be obtained. From the experimental results (Fig. 10) it can be noticed that water absorptions of the cubes (WA_c) and the hollow blocks (WA_b) were similar to each other in all the cases and that the values dropped with the increase in peak temperature. Water absorption in BC1 somewhat decreased with the firing temperature, which is caused by the nature of the raw material and the high content of finely dispersed carbonates. The mechanical characteristics of the hollow products are satisfying and similar to those presented in the literature related to the bricks without voids (Gökçe et al., 2018). There is a slight increase in mechanical characteristics with increasing the peak firing temperature. Compressive strengths differed significantly depending on the structure of the samples: hollow blocks with vertical voids showed about 2 – to 2.5 times lower values. The lowest WAs were found in BC2, while the highest were in the samples BC1 at various firing temperatures, and the situation was vice-versa in terms of the compressive strengths. Among the composites, the highest CSs and the lowest WAs were found in C5, the highest WAs were observed in the C3 samples, while the lowest CSs were determined in C1 and C2. All the samples shown WAs below the critical 20 % (Deraman et al., 2018; Muñoz et al., 2019; Özdemir and Sarici, 2020), while the composite brick clay-coal ash bricks showed somewhat lower values of water absorption than previously reported (Gökçe et al., 2018), concerning the lower quantity of the added coal dust. When comparing the results when using coal mines waste containing soil, the results on WA were significantly higher (Özdemir and Sarici, 2020), so as expected energy-efficiency of the newly obtained products.

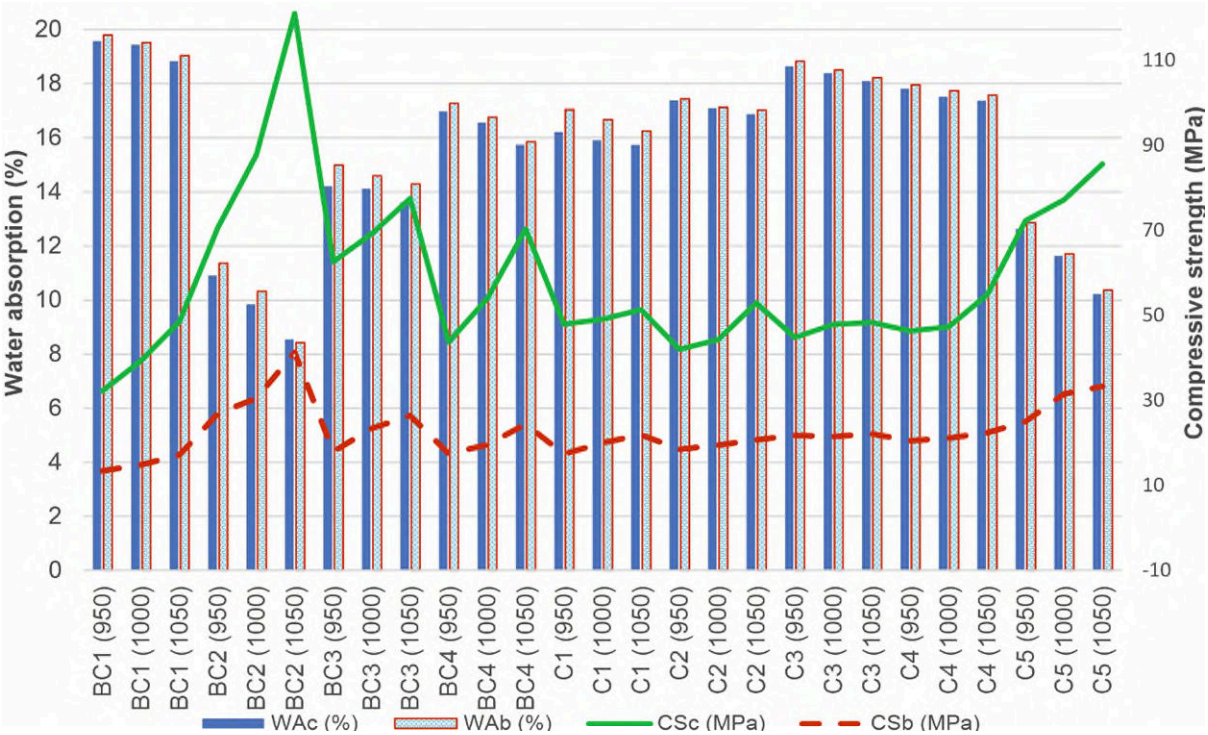

Fig. 10. Water absorption and compressive strength of the laboratory samples fired at 950 ºC, 1000 ºC, and 1050 ºC (WA_c - water absorption of cubes, WA_b -water absorption of hollow blocks, CS_c – compressive strength of cubes, CS_b – compressive strength of hollow blocks).

The highest mechanical characteristics of all the tested samples were shown by the samples marked C5, given that they contain the highest proportion of clay minerals and low content of carbonates. Since the deposits of loess soils are limited in the amount of more clayey sections, a combination of 70 % BC1 and 30 % BC2 was chosen for the optimal mixture of brick clays. This mixture lowers carbon-footprint when compared to firing BC1 type of clay alone (González et al, 2016). The possible decrease in carbon footprint, when using 97 wt.% of clay consisting of 9.8 % of total carbonates, is estimated to be about 0.3 %, which is a significant amount in industrial conditions. CD1 was chosen as a more suitable additive due to its higher calorific value. Considering the compressive strength and water absorption obtained in sample C3, the chosen amount of CD1 was 3 %. In the case of lower addition of the highly calcareous clay BC1 to the mixture (< 70 %), by using mass containing higher quantities of clay minerals, the increased addition of waste coal dust would be possible (4 % - 4.5 %).

487 *3.4. Firing regime of the industrial-scale products in a tunnel kiln*

488

489 The industrial probe is made based on the composite C3. The hollow blocks
490 with vertical voids of dimensions 250x190x190 mm^3 are extruded in the factory. The
491 samples that contained 1.84 % particles above 0.063 mm were of high plasticity,
492 moderate susceptibility to drying while drying shrinkage was 5.74 %. The registered
493 regime, expressed as a function of time, i.e. distance from the entrance to the tunnel
494 kiln, is shown in Fig.11a.

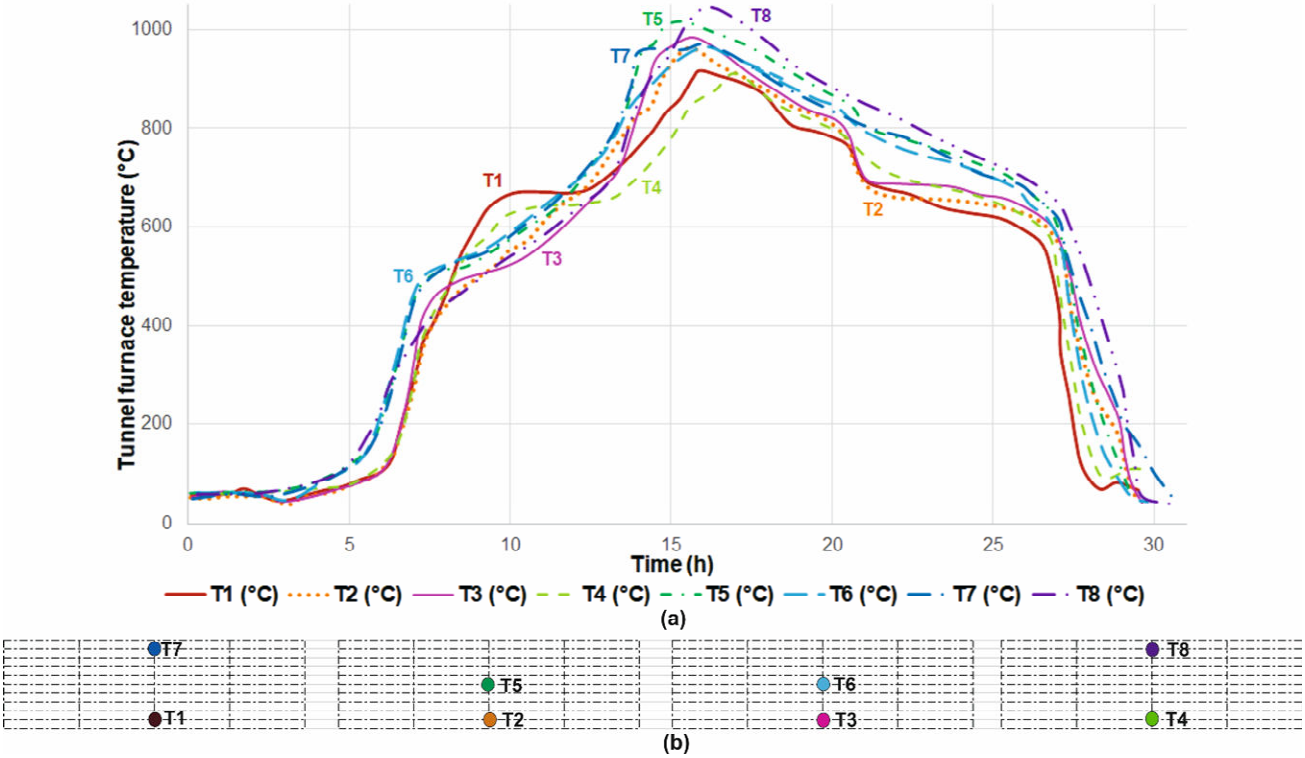

Fig. 11. (a) Firing regime in the tunnel kiln, (b) Position of thermocouples in the wagon (T1 – T8).

The wagon in the tunnel kiln contained 4x4 stacks with a height of 10 products (190 mm per product). The thrust was such that in 2 h the whole wagon entered the furnace. The frequency of data collection during the recording of the firing regime was 15 minutes for each thermocouple. The locations of the thermocouples during the acquisition of the firing regime were as shown in Fig.11b. Based on the results of the regime's diagnosing (Fig. 11) while subtracting the 2 h in which time the wagon entered the furnace, the duration of the main firing phases is shown in Table 4. It is seen that the lowest peak temperatures are registered at the bottom of the stacks, as expected. The difference between the measured maximum firing temperatures at bottom of the stacks was 140 °C. A difference in temperature (up to 160 °C) in the preheating zone was registered along with the height of the fire channel. It is determined that in some positions of the stack, during both the firing and the cooling zone, the temperature differences were too high (up to 180 °C). The differences in the temperature within the tunnel kiln mean that the quality of products is not uniform. Some of the samples can be lighter in color and not satisfyingly fired, while the others may be over-fired. The lowest peak temperatures were detected in lower positions of the stack due to the air

circulating under the wagons and not such a good sealing by using sand (Nicolau and Dadam, 2009).

Table 4

Duration of the firing phases and maximum peak temperatures as per thermocouples measurements (T1 – T8).

Thermocouple	Preheating zone (to 750 °C) (h)	Firing zone (750 °C-1045 °C) (h)	Cooling zone (h)	Total time in the kiln (h)	Maximum peak temperature (°C)
T1	11.93	6.60	9.30	27.83	905
T2	10.83	7.67	9.33	27.83	967
T3	11.43	7.10	9.30	27.83	990
T4	12.27	7.17	8.40	27.83	911
T5	10.63	9.87	7.33	27.83	1016
T6	11.08	9.80	6.95	27.83	964
T7	10.67	9.70	7.47	27.83	967
T8	11.17	10.08	6.58	27.83	1045

The preheating phase was satisfactorily led, considering the low sensitivity for cracks of loess clays in this period (low drying shrinkage and moderately sensitive nature in drying). The length of the preheating stage was good (approximately 11 - 12 hours), as in previous studies (Remmey, 1994; Vasić et al., 2017). The firing phase included significant differences in the peak temperatures and time of retention at different positions, and thus must be corrected. The firing phase lasted up to 10 h but should be prolonged to about 12 h especially because of the addition of the waste coal dust (Vasić et al., 2017). The proposed optimal firing temperature in the tunnel kiln is 950 °C. The cooling phase lasted up to 9.3 h and must be prolonged to about 12 h. The phase of slow cooling must be led bearing in mind the phase transformation of quartz (620 °C – 520 °C) when the cooling speed should be of 20 °C/h – 30 °C/h (Nicolau and Dadam, 2009; Vasić et al., 2017). The period of slow cooling in the tunnel kiln has shifted to temperatures higher than 575 °C. The goods in all positions reached

575 °C during the period of final intensive cooling when the cooling velocity was 20 °C/min – 25 °C/min. The complete firing process should last for about 36 h, which is much shorter than the one needed for other types of clays (Vasić et al., 2017), which makes these clays suitable and economically practical.

At the temperatures above 800 °C, products spent between 4.4 h - 8.9 h; above 850 °C, products spent 2.6 h - 7.0 h; and above 900 °C, the products spent 0.0 to 3.9 hours in different positions. At positions T1 and T4, products did not even reach 900 °C. The temperature of 1000 °C was reached by the products in two positions. The cooling zone is not adapted to the period of phase transformation of quartz when the products are sensitive due to large volume change.

3.5. Quality of industrial products

After the extrusion process, 3 moist blocks from the brick kiln were taken and tested in the laboratory. It is determined that drying shrinkage was 0.24 % while firing shrinkage, LOI, and water absorption after firing in the electric furnace were -0.21 %, 12.32 %, and 20.33 % respectively. The conditions of drying and firing were as mentioned in *Section 2.3*.

After the correction of the firing regime in the tunnel kiln, the products were tested in the laboratory for compressive strength and water absorption determination in different positions of the stack (Table 5). The samples are marked according to the positions of the thermocouples (Fig. 11b).

It is seen that the differences in temperatures at the recorded positions in the height of the stack and between the left and right sides of the kiln were still high. Besides, the cooling zone was very unfavorable for the positions T5 and T6 (in the middle) during the quartz transformation phase. For position T1 (bottom left), the quartz transformation phase is at the transition between slow and final rapid cooling. For position S4 (bottom right) the quartz transformation phase is in the middle of slowed cooling. The average compressive strength of the tested blocks is satisfactory and was 11.1 MPa, which was higher than reported earlier in the industrial waste-added products (Munir et al., 2018), though a significant scattering of the results was observed. Low values of the compressive strengths (less than 10 MPa) were obtained for blocks from the middle of the stack were caused by fast cooling in the quartz transformation zone and high heating speed in the heating zone from 300 °C to 600

569 °C. This part of the regime should be slowed down to allow complete combustion of
570 the organic material before the appearance of the liquid phase in the clay mass. The
571 compressive strength of the tested blocks from the lower rows was satisfactory (10.2
572 MPa - 12.5 MPa) comparing to that of relatively low content of clay minerals blocks
573 (Mylan et al., 2017). The water absorption of these blocks was up to about 18 %.
574 Despite satisfactory compressive strengths, these products are considered underfired,
575 since LOI was low (3.7%). The compressive strength of the tested blocks from the
576 upper rows was satisfactory and amounts to 10.9 MPa to 11.1 MPa. The water
577 absorption of the blocks fired in the upper rows was about 18 %.
578
579 **Table 5**
580 Important characteristics of the waste coal dust samples.

	Water absorption (%)	Compressive strength (MPa)	Peak temperature (°C)
Sample T1	18.11	12.5	850
Sample T2	17.68	12.5	805
Sample T3	17.48	11.4	747
Sample T4	17.83	10.2	720
Sample T5	19.21	9.9	920
Sample T6	19.32	9.3	896
Sample T7	19.10	11.1	988
Sample T8	19.15	10.9	953

581
582 **4. Conclusions**
583
584 This study was the first of a kind examination of the usability of waste coal
585 dust in fired brick production at several levels. Initially, mixtures of clays and various
586 samples of waste coal dust were tested at the laboratory level to determine the mineral
587 and chemical composition, behavior during heating, shaping, drying, and finally,
588 properties of the products fired between 950 °C and 1050 °C are reported. It is
589 determined that the low quantities of waste coal dust introduced high changes to the
590 quality of the laboratory products. It was estimated that the addition of highly caloric
591 waste coal dust of 3 % is optimal for the given conditions and that by mixing with loess
592 clay, energy-efficient products are created. The compressive strength of the hollow
593 laboratory blocks (50 % of voids) made of the optimal mix was around 22 MPa, while
594 water absorption was between 18.2 % and 18.8 %.

The selected mixture was then used to make an industrial probe. The estimated quantity of waste coal dust to be spent daily in the production of 60,000 pieces of 250x190x190 mm^3 blocks is 12.5 t. In parallel with the assessment of the suitability of the mixture in industry, the firing regime in the tunnel kiln was recorded. It is determined that in some positions of the stack, during both the firing and the cooling zone, the temperature differences were too high (up to 180 °C). The differences in the temperature within the tunnel kiln mean that the quality of products is not uniform. Some of the samples can be lighter in color and not fired enough, while the others may be over-fired. The lowest peak temperatures were detected in lower positions of the stack due to the air circulating under the wagons and not such a good sealing by using sand (Nicolau and Dadam, 2009). After the correction of the regime, the quality of the obtained samples was found to be satisfactory.

Further investigations in terms of defining the durability of the obtained products by thaw-freezing tests, then thermal conductivity, and also the determination of leaching of heavy metals are the subjects of the upcoming study.

Acknowledgments

This study was supported by the Ministry of Education, Science and Technological Development of the Republic of Serbia (Contract No. 451-03-68/2020-14/200012). GG is particularly thankful to the Royal Academy of Engineering, UK to extend financial support via the Indo-UK partnership Industry-academia scheme (Grant No. IAPP18-19\295) with a follow-on funding under the auspices of the Engineering Pandemic preparedness program (EXPP2021\1\277).

References

Abi, E., F. Oruç, E. Sabah, 2011. Utilization of waste clay from coal preparation tailings for brick production. J. Ore Dress. 13 (25), 22-32.

Arsenović, M., Pezo, L., L. Mančić, Radojević, Z., 2014. Thermal and mineralogical characterization of loess heavy clays for potential use in brick industry. Thermochim. Acta 580, 38–45. https://doi.org/10.1016/j.tca.2014.01.026

Arsenović, M., Radojević, Z., Jakšić, Ž., Pezo, L., 2015a. Mathematical approach to application of industrial wastes in clay brick production – Part I: Testing and

analysis. Ceram. Int. 41(3) 4890 - 4898. https://doi.org/10.1016/j.ceramint.2014.12.051

Arsenović, M., Radojević, Z., Jakšić, Ž., Pezo, L., 2015b. Mathematical approach to application of industrial wastes in clay brick production – Part II: Optimization. Ceram. Int. 41(3), 4899-4905. https://doi.org/10.1016/j.ceramint.2014.12.050

Bocanegra, J.J.C., Mora, E.E., González, G.I.C., 2019. Galvanic sludges: Effectiveness of red clay ceramics in the retention of heavy metals and effects on their technical properties. Environ. Technol. Innov. 16, 100459. https://doi.org/10.1016/j.eti.2019.100459

Chen, X., Zhang, Y., Zhang, Q., Li, C., Zhou, Q., 2015. Thermal analyses of the lignite combustion in oxygen-enriched atmosphere. Therm. Sci. 19 (3), 801 - 811. https://doi.org/10.2298/TSCI141005007C

Cobo-Ceacero, C.J., Cotes-Palomino, M.T., Martínez-García, C., Moreno-Maroto, J.M., Uceda-Rodríguez, M., 2019. Use of marble sludge waste in the manufacture of eco-friendly materials: applying the principles of the Circular Economy. Environ. Sci. Pollut. Res. 26, 35399–35410. https://doi.org/10.1007/s11356-019-05098-x

Deraman, R., Abdullah, A.H.b., Nagapan, S., Abas, N.H., Suratkon, A.B., Hasmori, M.F., 2018. Improving thermal conductivity of fired clay brick using sawdust waste. Asian Journal of Technical Vocational Education And Training (AJTVET) 4 (2018) 1-8.

Fan, G., Zhang, D., Wang, X., 2014. Reduction and utilization of coal mine waste rock in China: A case study in Tiefa coalfield. Resour. Conserv. Recycl. 83, 24– 33. http://dx.doi.org/10.1016/j.resconrec.2013.12.001

Ferrer, S., Mezquita, A., Gomez-Tena, M.P., Machi, C., Monfort, E., 2015. Estimation of the heat of reaction in traditional ceramic compositions. Appl. Clay Sci. 108, 28-39. https://doi.org/10.1016/j.clay.2015.02.019

Goel, G., Kalamdhad, A.S., Agrawal, A., 2018. Parameter optimisation for producing fired bricks using organic solid wastes. J. Clean. Prod. 205, 836-844. https://doi.org/10.1016/j.jclepro.2018.09.116

Gökçe, M.V., Akçaözoğlu, S., Sinani, B., 2018. Investigation of production of brick with waste coal powder additive. Proceedings of the 7th annual international conference, International conference on civil engineering, infrastructure and environment, UBT Innovation campus, 26.-28. October 2018, 39-47.

González, I., Barba-Brioso, C., Campos, P., Romero, A., Galan, E., 2016. Reduction of CO_2 diffuse emissions from the traditional ceramic industry by the addition of Si-Al raw material. J. Environ. Manage. 180, 190-196. http://dx.doi.org/10.1016/j.jenvman.2016.05.039

Gupta, N., Gedam, V.V., Moghe, C., Labhasetwar, P., 2017. Investigation of characteristics and leaching behavior of coal fly ash, coal fly ash bricks and clay bricks. Environ. Technol. Innov. 7, 152-159. http://dx.doi.org/10.1016/j.eti.2017.02.002

Haibin, L., Zhenling, L., 2010. Recycling utilization patterns of coal mining waste in China. Resour. Conserv. Recycl. 54, 1331–1340. https://doi.org/10.1016/j.resconrec.2010.05.005

Kovács, B., Czinkota, I., Tolner, L., Czinkota, G.Y., 2006. FIT method for calculating soil particle size distribution from particle density and settling time data. Agrokémia és talajtan 55 (1), 295 – 304. https://doi.org/10.1556/agrokem.55.2006.1.32

Lemeshev, V.G., Gubin, I.K., Savel'ev, Y.A., Tumanov, D.V., Lemeshev, D.O., 2004. Utilization of coal mining waste in the production of building ceramic materials. Glass Ceram. 61 (9–10), 308-311. DOI: 10.1023/B:GLAC.0000048698.58664.97

Li, J., Wang, J., 2019. Comprehensive utilization and environmental risks of coal gangue: A review. J. Clean. Prod. 239, 117946. https://doi.org/10.1016/j.jclepro.2019.117946

Lingam, R.K., Suresh, A., Dash, P.S., Sriramoju, S.K., Ra, T., 2016. Upgrading coal washery rejects through caustic-acid leaching. Min. Proc. Ext. Met. Rev. 7:2, 69-72. https://doi.org/10.1080/08827508.2015.1115987

Mekki, H., Anderson, M., Benzina, M., Ammara, E., 2008. Valorization of olive mill wastewater by its incorporation in building bricks. J. Hazard. Mater. 158, 308-315. https://doi.org/10.1016/j.jhazmat.2008.01.104

Munir, M.J., Kazmi, S.M.S., Wu, Y.-F., Hanif, A., Khan, M.U.A., 2018. Thermally efficient fired clay bricks incorporating waste marble sludge: An industrial-scale study. J. Clean. Prod. 174, 1122-1135. https://doi.org/10.1016/j.jclepro.2017.11.060

694 Muñoz, P., Mendívil, M.A., Letelier, V., Morales, M.P., 2019. Thermal and mechanical
695 properties of fired clay bricks made by using grapevine shoots as pore forming
696 agent. Influence of particle size and percentage of replacement. Constr. Build.
697 Mater. 224, 639-658. https://doi.org/10.1016/j.conbuildmat.2019.07.066
698 Mylan, R., Maharaj, C., Maharaj, R., 2017. Creating the optimal product formula for
699 use by a heavy clay block manufacturer. Clay Res. 35 (2), 71-83.
700 Nicolau, V. de P., Dadam, A.P., 2009. Numerical and experimental thermal analysis
701 of a tunnel kiln used in ceramic production. J. of the Braz. Soc. of Mech. Sci.
702 & Eng. XXXI (4), 297-304. https://doi.org/10.1590/S1678-
703 58782009000400003
704 Nigay, P.M., Cutard, T., Nzihou, A., 2017. The impact of heat treatment on the
705 microstructure of a clay ceramic and its thermal and mechanical properties,
706 Ceram. Int. 43(2), 1747–1754. https://doi.org/10.1016/j.ceramint.2016.10.084
707 Ozbas, E., Kök, M.V., Hicyilmaz, C., 2003. DSC study of the combustion properties
708 of Turkish coals. J. Therm. Anal. Calorim. 71, 849–856.
709 https://doi.org/10.1023/A:1023378226686
710 Özdemir, E., Sarici, D.E., 2020. Estimation of calorific values of some of the Turkish
711 lignites by Artificial Neural Network and Multiple Regressions. Curr. Phys.
712 Chem. 10, 1-9. https://doi.org/10.2174/1877946809666191120125450
713 Pontikes, Y., Rathossi, C., Nikolopoulos, P., Angelopoulos, G.N., Jayaseelan, D.D.,
714 Lee, W.E., 2009. Effect of firing temperature and atmosphere on sintering of
715 ceramics made from Bayer process bauxite residue. Ceram. Int. 35, 401–407.
716 https://doi.org/10.1016/j.ceramint.2007.11.013
717 Rekecki, R., Ranogajec, J., Oszkó, A., Kuzmann, E., 2004. Effects of firing conditions
718 on the properties of calcareous clay roofing tiles. J. Mater. Civ. Eng. 26(1),
719 175-183. https://doi.org/10.1061/(ASCE)MT.1943-5533.0000783
720 Remmey, G.B., 1994. Firing ceramics, Advanced Series in Ceramics, Vol. 2, World
721 Scientific.
722 Rimpel, E., 2019. Tunnel kiln: Technology overview and project assessment
723 guideline. Remmey, G.B., 1994. Firing ceramics, Advanced Series in
724 Ceramics, Vol. 2, World Scientific. Available at:
725 https://www.ccacoalition.org/en/resources/tunnel-kiln-technology-overview-
726 and-project-assessment-guideline

727 Soussi, N., Kriaa, W., Mhiri, H., Bournot, P., 2017. Reduction of the energy
728 consumption of a tunnel kiln by optimization of the recovered air mass flow
729 from the cooling zone to the firing zone. Appl. Therm. Eng. 124, 1382-1391.
730 http://dx.doi.org/10.1016/j.applthermaleng.2017.06.111
731 SRPS EN 772-1 Methods of test for masonry units - Part 1: Determination of
732 compressive strength, Institute for standardization of Serbia, Belgrade, 2016.
733 SRPS U.B1.018 Testing of soils - Determination of particle size distribution, Institute
734 for standardization of Serbia, Belgrade, 2005.
735 SRPS EN 772-13 Methods of test for masonry units - Part 13: Determination of net
736 and gross dry density of masonry units (except for natural stone), Institute for
737 standardization of Serbia, Belgrade, 2010.
738 SRPS EN 772-21 Methods of test for masonry units - Part 21: Determination of water
739 absorption of clay and calcium silicate masonry units by cold water absorption,
740 Institute for standardization of Serbia, Belgrade, 2012.
741 Stolboushkin, A.Yu., Ivanov, A.I., Fomina, O.A., 2016. Use of coal-mining and
742 processing wastes in production of bricks and fuel for their burning. Procedia
743 Eng. 150, 1496 – 1502. https://doi.org/10.1016/j.proeng.2016.07.089
744 Taalab, A.S., Ageeb, G.W., Siam, H.S., Mahmoud, S.A., 2019. Some characteristics
745 of calcareous soils. A review. Middle East J. Agric. Res. 8(1), 96-105.
746 Taha, Y., Benzaazoua, M., Hakkou, R., Mansori, M., 2016. Coal mine wastes
747 recycling for coal recovery and eco-friendly bricks production. Miner. Eng.
748 107, 123-138. http://dx.doi.org/10.1016/j.mineng.2016.09.001
749 Vasić, M., Pezo, L., Radojević, Z., 2020. Optimization of adobe clay bricks based on
750 the raw material properties (mathematical analysis). Constr. Build. Mater. 244,
751 118342. https://doi.org/10.1016/j.conbuildmat.2020.118342
752 Vasić, M.V., Pezo, L., Zdravković, J.D., Bačkalić, Z., Radojević, Z., 2017. The study
753 of thermal behavior of montmorillonite and hydromica brick clays in predicting
754 tunnel kiln firing curve. Constr. Build. Mater. 150, 872-879.
755 https://doi.org/10.1016/j.conbuildmat.2017.06.068
756 Vasić, M.V., Pezo, L., Zdravković, J.D., Vrebalov, M., Radojević, Z., 2018. Thermal,
757 ceramic and technological properties of clays used in production of roofing
758 tiles – Principal Component Analysis. Sci. Sinter. 50 (4), 487-500.
759 https://doi.org/10.2298/SOS1804487V

760 Vijayan, D.S., Parthiban, D., 2020. Effect of Solid waste based stabilizing material
761 for strengthening of Expansive soil- A review. Environ. Technol. Innov. 20,
762 101108. https://doi.org/10.1016/j.eti.2020.101108
763 Vukićević, M., Popović, Z., Despotović, J., Lazarević, L., 2018. Fly ash and slag
764 utilization for the Serbian railway substructure transport. Transport 33(2), 389–
765 398. https://doi.org/10.3846/16484142.2016.1252427
766 Weng, C.H., Lin, D.F., Chiang, P.C., 2003. Utilization of sludge as brick materials,
767 Adv. Environ. Res. 7. 679–685. http://dx.doi.org/10.1016/S1093-
768 0191(02)00037-0